Signatures of stratosphere to troposphere transport near deep convective events in the southern subtropics

Jimmy Leclair de Bellevue, Anne Réchou, Jean-Luc Baray, Gérard Ancellet, R.-D. Diab

Signatures of stratosphere to troposphere transport near deep convective events in the southern subtropics

J. Leclair De Bellevue,[1] A. Réchou,[1] J. L. Baray,[1] G. Ancellet,[2] and R. D. Diab[3]

Received 5 December 2005; revised 20 June 2006; accepted 25 August 2006; published 20 December 2006.

[1] A climatology of tropospheric ozone profiles associated with tropical convection in the southwestern part of the Indian Ocean and over South Africa is presented. Then case studies of stratospheric-tropospheric exchange are documented using radiosoundings, ozone lidar, satellite and ECMWF global model data. In three distinct cases of varying tropical convection intensity (depression and cyclone Guillaume near Reunion in February 2002 and convection near Irene in November 2000), strong interaction between convection-induced upper level circulation, jet front systems and Rossby Wave Breaking induces stratosphere to troposphere exchanges. Stratospheric filaments in the upper troposphere evident in the ECMWF analyses are in good agreement with ozone, humidity and temperature vertical profile observations. For the Guillaume case study near Reunion, filaments and subsidence occur in both cases (depression on 15 February and cyclone on 19 February 2002). On 15 February, a moderate enhancement of ozone in the free troposphere is observed and on 19 February, a 100 ppbv ozone peak is recorded. In the Irene case study, a large upper level depression coming from the stratosphere, fed by a filament wrapped around the convective area in the Mozambican channel, induces an ozone peak of larger magnitude (170 ppbv). Secondary ozone sources (jet front system in the Atlantic and biomass burning in South America) could further amplify this ozone enhancement. The radiosounding indicates a strong ozone enhancement in the upper troposphere, without a signature of pumping from the lower layers, in contrast to the Guillaume case.

Citation: Leclair De Bellevue, J., A. Réchou, J. L. Baray, G. Ancellet, and R. D. Diab (2006), Signatures of stratosphere to troposphere transport near deep convective events in the southern subtropics, *J. Geophys. Res.*, *111*, D24107, doi:10.1029/2005JD006947.

1. Introduction

[2] The understanding of the transport of trace chemical species between the stratosphere and the troposphere is necessary for global change prediction. Tropospheric ozone is a minor component of the atmosphere which plays an important part in the photochemical balance of the troposphere, because of its high oxidizing potential with other chemical species. Moreover, changes in the vertical distribution of ozone, a greenhouse gas, influence the atmospheric radiative balance. Two main mechanisms explain high ozone concentration in the upper levels of the troposphere: photochemistry (pollution, biomass burning) and stratospheric-tropospheric exchange (STE).

[3] In the tropics, earlier studies of tropospheric ozone suggested that the ozone budget is controlled primarily by biomass burning which injects ozone precursors into the troposphere [*Fishman et al.*, 1990; *Browell et al.*, 1996; *Fujiwara et al.*, 1999; *Randriambelo et al.*, 2000; *Thompson et al.*, 2003].

[4] More recent studies indicate that STE, induced by the subtropical jet stream or by Rossby Wave Breakings (RWB), could also contribute significantly to tropospheric ozone enhancement [*Scott et al.*, 2001; *Gouget et al.*, 1996; *Folkins and Appenzeller*, 1996].

[5] Indeed, tropospheric ozone inputs could also result from convection induced downdraughts. Apart from its role in upward transport and diffusion of chemical species produced by biomass burning, the influence of convection on tropospheric ozone is complex and includes both dynamical and chemical components. Owing to mass conservation, convection-induced dynamical influences are not likely to be limited to upward lifting of ozone-poor air from lower layers of the troposphere. Detrainment of air is expected to play some part in the tropospheric ozone budget [*Chatfield and Crutzen*, 1984; *Dickerson et al.*, 1987; *Thompson et al.*, 1996]. Ozone measurements have been performed regularly at Reunion (20.8°S, 55.5°E) since 1992 [*Baldy et al.*, 1996]. At Irene (25.9°S, 28.2°E), located in South Africa [*Diab et al.*, 1996, 2004], soundings were taken in 1990–1993 and again from 1998 to the present. A first case study of convection-induced downdraughts injecting a high concentration of ozone in the troposphere has

[1] Laboratoire de l'Atmosphère et des Cyclones, CNRS-UMR 8105, Université de La Réunion, La Réunion, France.
[2] Service d'Aéronomie, CNRS-UMR 7620, Université Pierre et Marie Curie, Paris, France.
[3] School of Environmental Sciences, Howard College Campus, University of KwaZulu-Natal, Durban, South Africa.

0148-0227/06/2005JD006947

Table 1. Number of Tropospheric Ozone DIAL Nighttime Measurements and Radiosounding Performed by Year Since 1995

Year	Lidar Acquisitions	Ozonesondes
1995	...	18
1996	...	17
1997	...	25
1998	35	35
1999	32	49
2000	17	39
2001	4	28
2002	30	30
2003	23	18
2004	51	41

been presented by *Baray et al.* [1999a]. This high ozone enhancement attributed to tropical cyclone Marlene has also been observed in the pre-INDOEX (Indian Ocean Experiment) campaign [*De Laat et al.*, 1999; *Baray et al.*, 2001].

[6] In this paper, in order to improve our understanding of deep convection- or tropical cyclone- induced downdraughts and STE, we first demonstrate that STE induced by cyclones is quite frequent and propose an approach to assess its impact on ozone profiles. Then, the variability of STE signatures, observed on O_3, H_2O, and potential vorticity (PV) for two case studies will be analyzed in relation to the upper troposphere circulation induced by tropical convection.

[7] In section 2, we describe the data set used in the paper. The influence of cyclonic systems on ozone climatology is presented in section 3. Section 4 focuses on case study analyses and the concluding discussion is given in section 5.

2. Data Set

2.1. In Situ Data

[8] This paper is based on two types of in situ data. The first type is combined PTU-ozone soundings (PTU is from the radiosonde and attached to it during flight is the separate ozonesonde) performed at Irene and Reunion. The second in situ data come from a tropospheric ozone lidar operating at Reunion.

[9] The soundings provide vertical profiles of ozone, relative humidity and temperature from the ground to around 30 km. The balloon-borne device used at Irene was a Science Pump ECC (electrochemical concentration cell) Type 6A ozonesonde with a Vaisala radiosonde. At Reunion both Science Pump Type 6A and EnSci Z-type ozonesondes have been used [*Thompson et al.*, 2003]. The accuracy of these devices has been evaluated in field and chamber tests [*Barnes et al.*, 1985; H. J. G. Smit et al., Assessment of the performance of ECC-ozonesondes under quasi-flight conditions in the environmental simulation chamber: Insights from the Julich Ozone Sonde Intercomparison Experiment (JOSIE), submitted to *Journal of Geophysical Research*, 2006]. The vertical resolution of the data is around 50 meters. Irene and Reunion are part of the SHADOZ (Southern Hemisphere Additional Ozonesondes) network [*Thompson et al.*, 2003] and the sonde data used here are available at http://croc.gsfc.nasa.gov/shadoz.

[10] The measurements of tropospheric ozone by the lidar system are made by differential absorption in the ultraviolet wavelength band (289–316 nm). These wavelengths are obtained by stimulated Raman scattering of the fourth harmonic of the Nd-Yag laser beam in deuterium. The lidar altitude range is typically from 3 km to around 15 km, the upper limit depending on the meteorological conditions and ozone amount. The altitude resolution of the final ozone profiles is 15 m for the analog signal (from 3 to 6–7 km), and 150 m for the photon counting signal (from 6–7 km to the upper limit). Technical details of the system and validation are given by *Baray et al.* [1999b].

[11] Both types of measurements are currently operational and the number of profiles recorded by each system is given in Table 1.

2.2. Satellite Data

[12] Geostationary satellite images from METEOSAT are used in this study**.** Currently, EUMETSAT (Europe's Meteorological Satellite Organization) is operating Meteosat satellites at positions of 63°E (Meteosat 5) and 0° longitude (Meteosat 7). For the Zero Degree Service browse images are available every 6 hours (0000, 0600, 1200 and 1800 UT). For the Indian Ocean Data Coverage Service (IODC) (images from 63°E) images are available every 3 hours. These are provided in three different channels: visible, thermal infrared and water vapor infrared (http://www.eumetsat.de).

2.3. Global Model Data and Back Trajectories

[13] The meteorological data (wind, humidity and PV) used in the present study are 6-hourly (0000, 0600, 1200 and 1800 UTC), on 60 vertical levels from routine analysis of the European Centre for Medium-Range Weather Forecasts (ECMWF). We used data with a horizontal resolution of 0.5°.

[14] Back trajectories were calculated by the Lagrangian particle dispersion model FLEXPART version 4.3 [*Stohl et al.*, 1998], which was used in several studies of long-range transport of trace substances [e.g., *Stohl and Trickl*, 1999]. The model uses ECMWF input fields with a horizontal resolution of 1°, at all 60 vertical model levels, and with a time resolution of 3 hours. Advection and turbulent dispersion are taken into account by calculating the trajectories of a multitude of parcels. Solving Langevin equations, stochastic fluctuations of the three wind components are superimposed on the grid-scale winds to represent transport by turbulent eddies. The convection scheme used in FLEXPART was developed by *Emanuel and Zivkovic-Rothman* [1999].

3. Tropospheric Ozone Climatology During the Cyclonic Season

[15] *Rodgers et al.* [1990], studying the undulatory adjustments near to tropical cyclones from simulations and TOMS data, observed a significant descent of the tropopause height in the eye and the peripheral areas of the cyclone.

[16] Links between ozone and tropical convection have been investigated in CEPEX (Central Equatorial Pacific Experiment): *Wang et al.* [1995], modeling a deep convective storm showed considerable stratosphere to troposphere

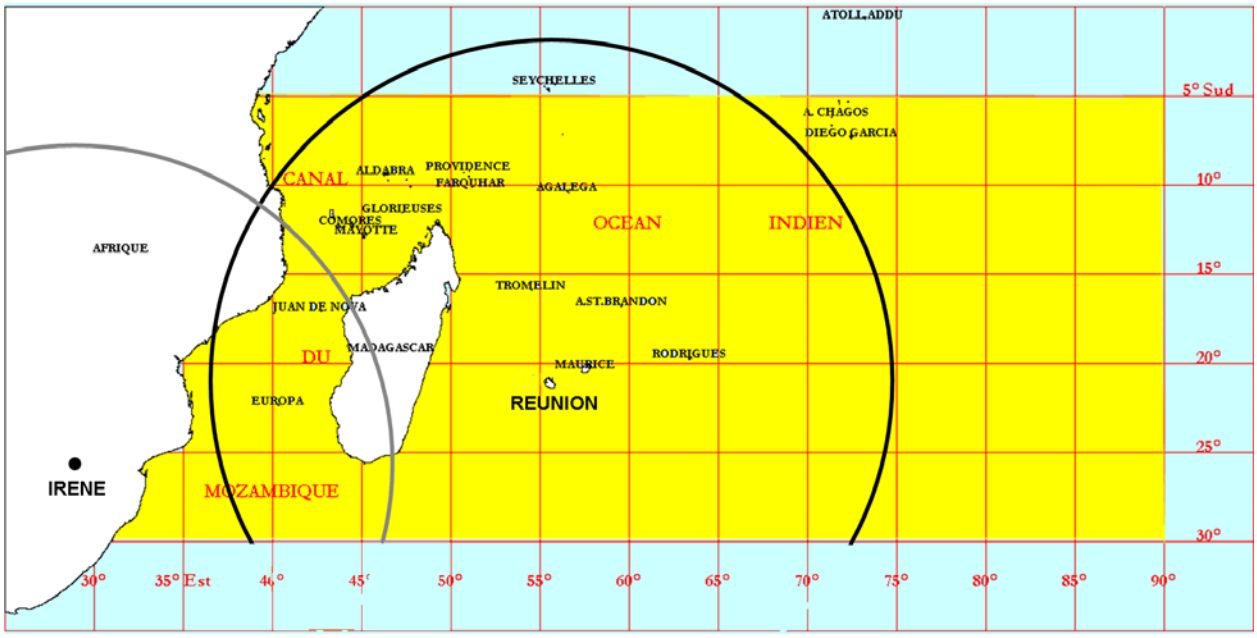

Figure 1. Cyclonic area of the southwestern Indian Ocean, depicted in yellow. The sampling of cyclonic systems for the climatological study is taken inside the geographical zones defined by a 2000 km radius around Reunion and Irene.

exchanges compared to upward exchanges in the convective tower.

[17] Analyzing data in the framework of TRACE-A, and carrying out statistical analysis of back trajectories, *Loring et al.* [1996] drew similar conclusions to those of *Rodgers et al.* [1990], published 6 years earlier.

[18] Other analyses showed that the vertical speeds induced by mesoscale convective clouds of the midlatitudes [*Stenchikov et al.*, 1996; *Poulida et al.*, 1996], during tropical convection events linked to the Inter Tropical Convergence Zone (ITCZ) [*Crutzen et al.*, 1979], and cumulonimbus clouds [*Mitra*, 1996] could play a role in the tropospheric ozone budget, by stratospheric-tropospheric exchange. Further, although large differences exist between tropical and midlatitudes cyclones, stratospheric ozone advection signatures into the troposphere are also found to accompany midlatitude cyclones [*Cooper et al.*, 2002].

[19] These recent studies showed that important subsidence could induce stratosphere to troposphere exchanges in the tropics, and that a dynamical link could exist between the cyclonic systems of tropical latitudes and tropospheric ozone distribution.

[20] According to the statistics available over 20 years, a global mean of 80–85 cyclonic events occur each year [*McBride*, 1995]. They are all localized at latitudes higher than 5°, and 87% of them occur within the tropics. The number of cyclones fluctuates from year to year, with a 10% standard deviation. However, strong interannual variability (15 to 70%) is observed when separate cyclonic regions are considered individually. Cyclonic activity fluctuates more in the northern Indian, the southwestern Pacific and the Atlantic Oceans than over the northwestern Pacific and the southwestern Indian Oceans. (The last one is our particular region of interest). Phenomena, such as the ENSO (El Nino Southern Oscillation) for the ocean and tropical troposphere and the QBO (Quasi Biennial Oscillation) for the low stratosphere, also influence the frequency of cyclones [*Gray*, 1979; *McBride*, 1995].

3.1. Cyclonic Activity in the Southwestern Indian Ocean

[21] The climatological study presented hereafter concerns the cyclonic area of the southwestern Indian Ocean using data from the Centre des Cyclones Tropicaux de La Réunion (CCTR). CCTR is a research center based at Reunion and keeps cyclonic data records. Figure 1 depicts the geographical delimitation of this area. The interannual variability of the cyclonic activity in the southwestern Indian Ocean region is illustrated in Figures 2 and 3.

[22] Figure 2 displays the temporal variation of cyclogenesis events (number of storms, depressions and tropical cyclones) by cyclonic season from 1992/1993 to 2003/2004, each season defined from 1 August to 31 July of the following year. The 1992/1993, 1993/1994 and 1996/1997 seasons have experienced greatest activity over this last decade, with 14, 15 and 14 cyclogenesis events respectively. In 1997/1998, 1998/1999 and 2000/2001, only 8 systems were observed in the region. It also appears that several consecutive active seasons are followed by seasons of reduced activity, as was the case between 1992/1993 and 1996/1997, when the number of events was equal to or greater than 11 systems per cyclonic season. Further, the seasons from 1997/1998 to 2001/2002 had an equivalent or lower activity than the mean over the period 1992 to 2004.

[23] The choice of seasonal period for the sampling of the cyclonic systems for the ozone climatology is an important criterion. Figure 3 shows monthly frequencies of systems based on the observations of 136 events (61 cyclones and 75 storms and depressions) between 1992 and 2004. The most common months for cyclones are from November to April (89% of the cyclonic activity), and hence examples for

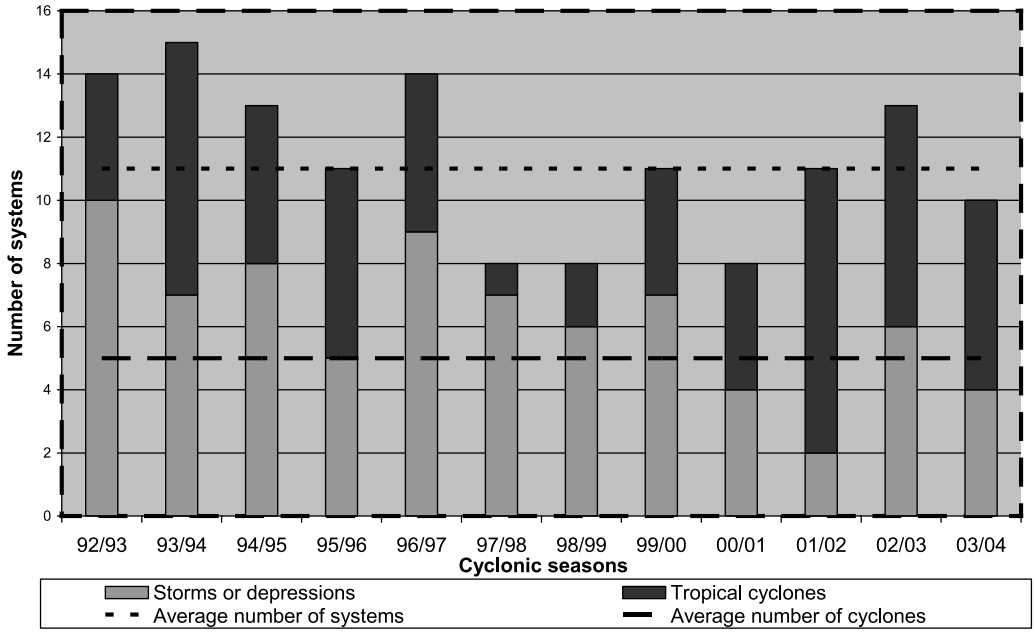

Figure 2. Interannual variability of storms, depressions and cyclones in the southwestern Indian Ocean during the 1992/1993 to 2003/2004 cyclonic seasons. The average is 11 systems and 5 cyclones per cyclonic season.

analysis are taken from this period. January and February experience 52% of the cyclonic activity. The sampling of systems in the ozone climatological study presented in section 3.2 relates to the period November to April.

3.2. Tropical Cyclonic Systems: Effects on the Mean Ozone Profiles

3.2.1. Methodology

[24] Two measurement sites, Reunion and Irene, are compared through the climatology based on radiosounding data from each station and the archives of CCTR. Reunion, located on the southern edge of the tropical zone, is well located for the study of exchanges related to tropical convection in summer, and the southerly movement of the ITCZ. Irene, in South Africa, which is more in the subtropics at 25.5°S, is less influenced by the ITCZ, and has a different geographical situation, being located 700 km from the coast, and at an altitude of 1523 m.

[25] The choice of the geographical area of radius 2000 km around each site is based on the assumption that the influence of convective systems beyond this threshold is not very significant. This dimension is higher than the

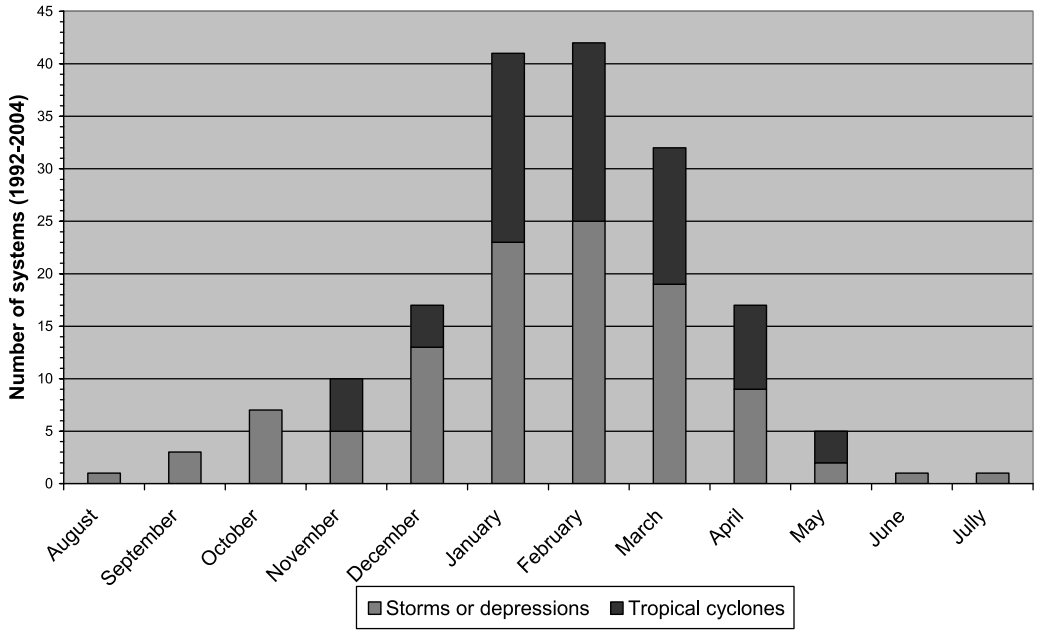

Figure 3. Seasonal frequency of cyclogenesis events in the southwestern Indian Ocean during 1992/1993 to 2003/2004 cyclonic seasons.

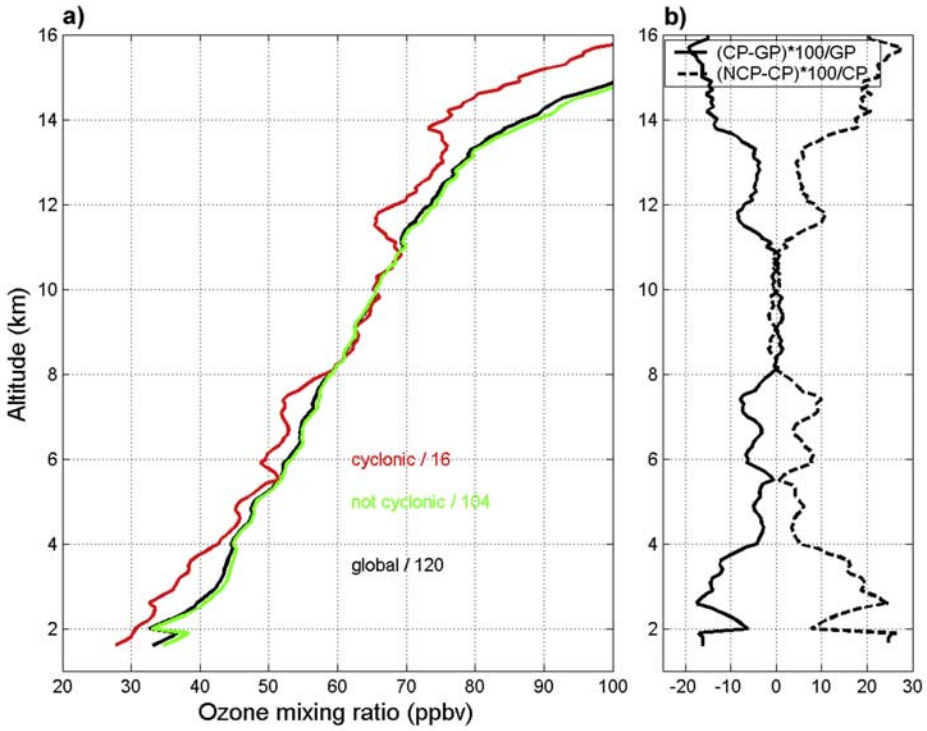

Figure 4. (a) Mean ozone mixing ratio profiles during November to April from 1998 to 2004, over Irene: ''cyclonic'' mean profile (red), ''noncyclonic'' profile (green) and global mean profile (black). The number of profiles used to calculate the mean profiles is indicated on the figure. (b) Relative deviation between cyclonic and global profiles (solid line) and between noncyclonic and cyclonic profiles (dashed line).

dimension of the most intense events. The number of systems of each cyclonic season is thus reduced by this criterion, from 136 to 112 around Reunion. Over the periods 1990 to 1993, and 1998 to 2003, 30 disturbances were observed in the geographical area of radius 2000 km around Irene. Most were over the southern part of the Mozambique Channel, with seven penetrating over the African subcontinent.

[26] The climatology of ozone profiles was first based on all ozone profiles measured for the months from November to April, for the period 1992 to 2004 at Reunion and 1990–1993, and 1998–2003 at Irene. On the basis of these data, a mean profile (GP) at each station for the cyclonic season was determined. Two classes of profiles were then distinguished: cyclonic (CP) and noncyclonic (NCP). The mean CP profile was calculated by using radiosoundings released during the active period of a cyclonic system and inside the 2000 km radius around the two sites. The mean NCP profile was calculated by using radiosoundings released without any cyclonic system in the 2000 km radius zone. A total of 94 profiles were obtained at Reunion during the cyclonic season; 59 of these profiles were cyclonic and 35 were noncyclonic. At Irene, 120 profiles were obtained during the cyclonic season, 16 being cyclonic and 104 noncyclonic.

3.2.2. Results

[27] Figure 4 depicts the three mean profiles above Irene. The relative difference between the cyclonic and noncyclonic profiles varies between 0 and +30% between 1 and 8 km altitude, whereas the relative difference between the cyclonic and global profiles varies between 0 and −20% over the same height interval. The cyclonic influence thus tends to decrease the mean ozone values, whereas the noncyclonic ozone values are higher than the mean global profile in the first 8 km of the troposphere. Between 8 and 11 km, the influence of the cyclonic systems on the mean ozone profile is not clearly discernible, and above 11 km, the cyclonic influence again tends to decrease the mean global ozone values.

[28] Figure 5a presents the three profiles for Reunion. The relative differences between the cyclonic and global profiles, and between the cyclonic and noncyclonic profiles are depicted in Figure 5b. The mean cyclonic profile exhibits a 0 to 5% enhancement over the mean global profile in the 3.5 km to 11.5 km altitude range, and up to a 5% reduction above 11.5 km. Compared with the mean noncyclonic profile, the differences are 0–20% and −15% to 0% between 3.5 km and 11.5 km respectively.

[29] It is clearly evident that the influence of cyclonic events on tropospheric ozone is much less structured and perceptible for Irene than for Reunion. This is due to the fact that, between 1998 and 2004, only 12 tropical cyclones occurred in the Mozambique Channel. Irene, which is situated far inland is less subject to the influence of these systems. In contrast, 112 systems were recorded in the 2000 km radial zone around Reunion. This oceanic site is thus potentially under the direct influence of these systems.

[30] The different geographical positions of Reunion and Irene thus explain the less visible influence at Irene. Moreover, the global mean ozone profile above Irene is

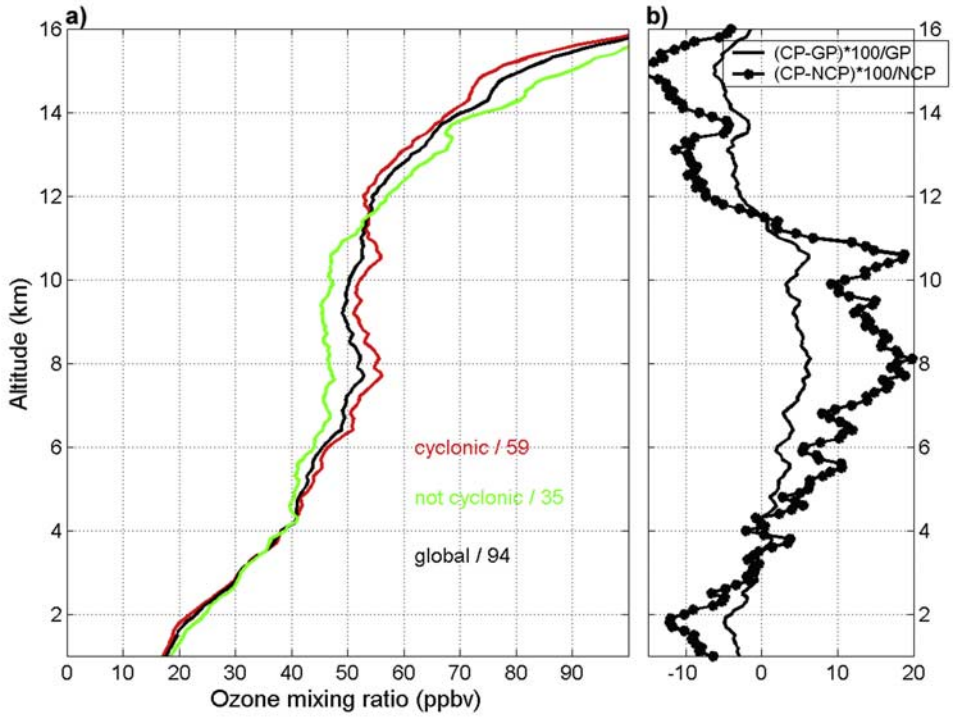

Figure 5. (a) Mean ozone mixing ratio profiles during November to April from 1992 to 2004, over Reunion: ''cyclonic'' mean profile (red), ''noncyclonic'' profile (green) and global mean profile (black). The number of profiles used to calculate the mean profiles is indicated on the figure. (b) Relative deviation between cyclonic and global profiles (solid line) and between cyclonic and noncyclonic profiles (dashed line).

close to typical midlatitude profiles. The climatological approach that we carried out by distinguishing the cyclonic from noncyclonic profiles underlines two effects of cyclonic systems on the ozone profiles, viz. an ozone enhancement in the midtroposphere and an ozone decrease in the upper troposphere. An hypothesis to explain this vertical ozone distribution would be the dual influence of convective systems (tropical storms, depressions and cyclones) on the climatology of tropospheric ozone: transfer of ozone from the stratosphere to the midtroposphere and a pumping of ozone-poor air masses from the boundary layer to the upper troposphere.

[31] An important outstanding question relates to the dynamical influences on the structure of the climatological ozone profiles during the cyclonic season.

[32] To further document exchanges near convective events, specific measurement campaigns have been undertaken [*Réchou et al.*, 2002], in addition to weekly routine ozone measurements. In the next section we present two case studies which can be considered as representative of the southern part of Africa and the southwestern Indian Ocean.

4. Case Studies of Stratospheric-Tropospheric Exchange Near Convective Events

4.1. Guillaume Event, February 2002

4.1.1. Observations

[33] Figure 6 depicts ozone, temperature and relative humidity profiles obtained on 15 and 19 February 2002, during the development of tropical cyclone Guillaume. The ozone profiles have been superimposed on the mean ozone profile and its associated variability calculated from 19 radiosoundings recorded at Reunion during the month of February since 1992.

[34] The 15 February ozone profile presents no strong ozone peak, but a large concentration of ozone in the entire upper troposphere (600 to 220 hPa). Between 350 and 150 hPa, the ozone mixing ratio is constant at $\sim$70 ppbv, about 20 ppbv above the climatological profile, corresponding to the upper limit of ozone variability in February. The ozonopause is at a low altitude (around 150 hPa, 15 km), indicated by a very sharp ozone increase (around 25 ppbv/km at 15 km). It is about 2 km below the thermal tropopause (-80°C at 17 km) depicted in Figure 6b. The fact that the ozonopause is below the thermal tropopause (the height where the vertical temperature gradient changes from a tropospheric value of about -6°C/km, to a stratospheric value of about $+3^{\circ}$C/km) means that there is ozone in the upper tropical troposphere, under the tropopause. This feature is sometimes observed at midlatitude sites in the Northern Hemisphere [*Bethan et al.*, 1996], and has been described by the concept of the Tropical Tropopause Layer (TTL) where the maximum altitude of deep convection does not reach the coldest temperature level [*Gettelman and Forster*, 2002].

[35] The profiles of relative humidity present large values in the lower layers (more than 80% between 0 and 3.5 km). The free troposphere is very dry (less than 20% until

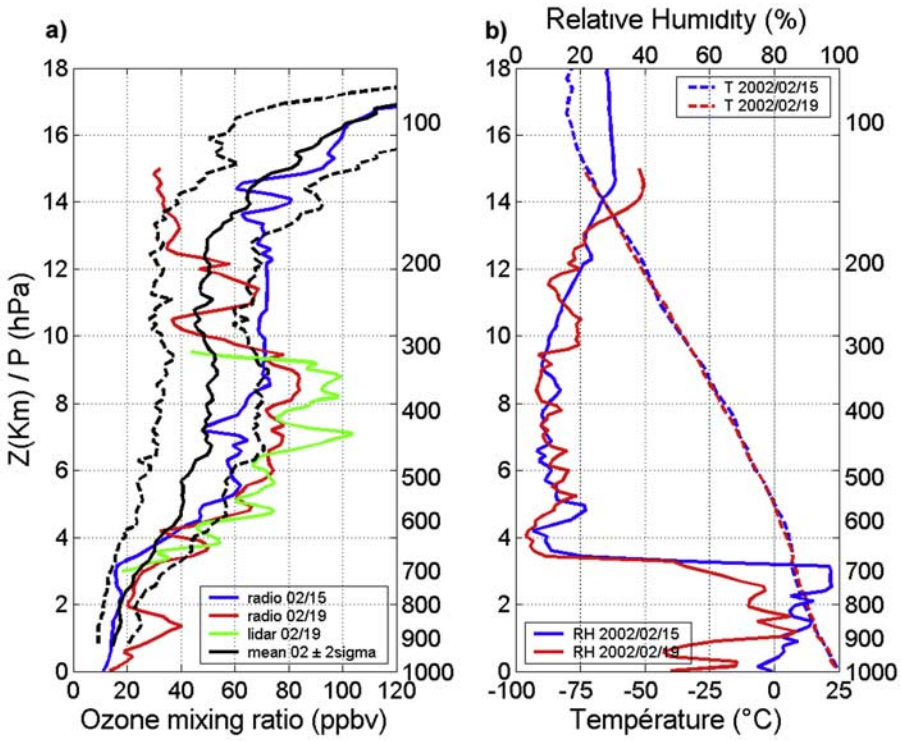

Figure 6. (a) Vertical profiles of ozone mixing ratio obtained by radiosounding over Reunion on 15 February 2002 at 1530 UT (blue), 19 February 2002 at 1300 UT (red) and by lidar profile between 1615 and 1650 UT (green), superimposed with a climatological profile of ozone for February (19 profiles from 1992 to 2002) (black line) and its standard deviation (black dashed lines). (b) Vertical profiles of relative humidity and temperature.

12.5 km). Nevertheless, because of the decreasing accuracy of the radiosounding sensor with altitude, humidity measurements in the upper troposphere can only be indicative.

[36] The two 19 February ozone profiles present an ozone peak at 350 hPa (83 ppbv for the radiosounding and 100 ppbv for the lidar). This peak is part of a larger ozone-enriched layer between 600 and 350 hPa. A negative ozone anomaly is observed in the upper levels (less than 40 ppbv at 275 hPa). The ozonopause is at a higher altitude than for the 15 February profile. This configuration has previously been observed when upper vertical motions affect the TTL by an overshoot of the deep convection.

[37] The 19 February ozone lidar profile was acquired three hours after the radiosounding. The upper limit of the profile was only 10 km, limited by the poor sky conditions during the cyclonic season (frequent clouds and high humidity). In the altitude range of the lidar (3–10 km), radiosounding and lidar profiles display the same structure, with peaks being more pronounced in the lidar profile. The 19 February relative humidity profile is very close to that recorded on 15 February, with a slightly less moist boundary layer (50 to 85% between 0 and 3.5 km).

4.1.2. Synoptic Situation

[38] We now highlight the synoptic context of this case study using Meteosat images (Figure 7). During the second half of February 2002, the Indian Ocean was affected by the convective system Guillaume. On 15 February, Guillaume was a convective zone without an apparent eye, and was detached from the ITCZ. The center was located near 16°S; 52°E, 750 km northwest of Reunion. On 19 February, the ITCZ moved northward. The convective depression Guillaume strengthened and became a cyclone. It was located near 18°S; 59°E, 350 km northeast of Reunion.

[39] Further, an upper level front was visible on the Meteosat image, about 2000 km southwest of Reunion. Two dry zones are evident on the water vapor images on 15 and 19 February, one located west of the front and the other located on the edge of Guillaume.

4.1.3. Temporal Evolution of the Air Masses

[40] Back trajectories ending over Reunion between 9.5 and 10.5 km on 15 and 19 February, 2002 display the history of the ozone-enriched air parcels (Figure 8). 120 hours before arriving over Reunion, the air mass was over the equatorial Atlantic Ocean. The air mass went southward, with subsidence occurring on 12 February, around 1200 UT (−75 hours) from altitudes of between 12.5 km and 13.5 km. This first subsidence was located in a northwesterly air stream over South Africa. An upward movement then occurred between −45 and −40 hours, and the trajectory moved northward, in the direction of Reunion. A second subsidence occurred on 14 February, around 0600 UTC (−30 hours) from a level of around 12.5 km (Figures 8a and 8b).

[41] In order to understand the origin of the air parcels, we used ECMWF wind and PV fields observed during this period (Figure 9). PV is a dynamical tracer frequently used in STE studies [*Hoskins*, 1991]. Despite some well known limitations of this tracer (diabatic production of PV in cyclones, its equatorial limit, and ECMWF data resolution

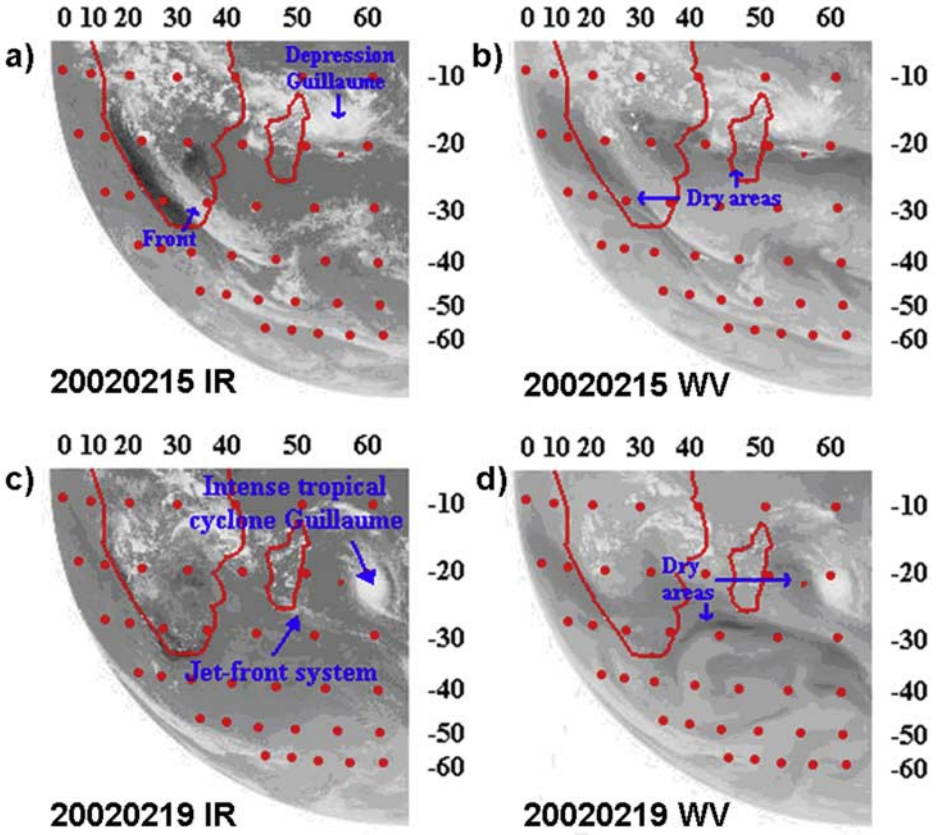

Figure 7. Meteosat-5 images on (a and b) 15 February and (c and d) 19 February at 1200 UT in the infrared (Figures 7a and 7c) and water vapor channels (Figures 7b and 7d).

mesoscale dynamics), we show hereafter that some significant characteristics are present.

[42] The first subsidence corresponds to the passage of the parcels in the jet front system above the Southern Atlantic on 12 February. The intense upward movement corresponds to the passage of the parcels in a strong anticyclonic curve of the jet stream over the southeastern coast of South Africa (Figure 8a), associated with a strong Rossby wave breaking (RWB hereafter) development in this region.

[43] RWB along the tropopause occurs preferentially during summer over the oceans, in relative proximity to the planetary-scale high-pressure systems in the subtropics [*Postel and Hitchman*, 1999]. These authors showed, using synoptic maps of RWB, that an acute tropopause folding in the meridional plane typically accompanies RWB. Some cases reveal the rich interaction between the tropical flow and the extratropical westerly current. The Guillaume case study showed a low-latitude penetration of the jet stream with the RWB, and a possible interaction between the RWB and the upper level circulation of Guillaume system.

[44] Just before arriving over Reunion, the trajectory indicates a second subsidence (Figures 8a and 8b). This second subsidence corresponds to the passage of the parcels in a high PV filament developing around the Guillaume system, and identified on the water vapor Meteosat image by a dry zone (Figure 7b). The trajectories arriving over Reunion between 8 and 9 km on 19 February 2002 have been calculated over 150 hours, i.e., beginning on 15 February (Figures 8c and 8d). Parcels present subsidence on 17 February around 0000 UT (−60 hours), linked to an almost southerly air stream. The long-term origin of some of the parcels (−150 hours) displays an important dispersion of the air masses, with a lower-tropospheric origin over Africa (between 10°E and 30°E and between 15°S and 20°S) for some parcels. The geographic area of this subsidence is the western and southwestern edge of the tropical cyclone area and corresponds to a cloudless and dry area on Meteosat images.

[45] Wind and absolute values of PV fields have been calculated at 340 K (275 hPa to 10 km) when the trajectories show clear subsidence, on 12, 14 and 17 February (Figure 9).

[46] The third subsidence described above seems to have the same dynamical origin as the first subsidence. However, on 17 February, no strong wind shear nor RWB occurred in the Mozambican channel, which explains why no strong upward movement has been observed.

[47] The parcels coming from the boundary layer could contribute to limit the magnitude of ozone peaks on 19 February, and induce some perturbations on the ozone profile of 19 February (Figure 6a), which presented some ozone-rich layers (at 7 and 9 km) and some ozone-poor layers (at 6.5, 7.5 and 10.5 km).

[48] When the Rossby wave moves eastward, the tongue of PV separates from the cyclone and the filament in the

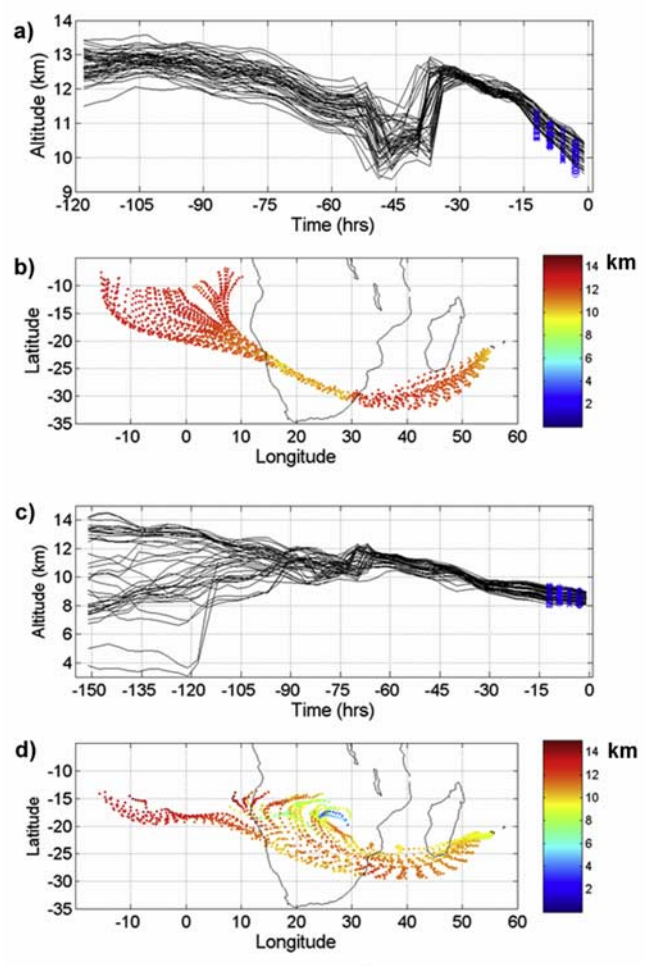

Figure 8. Cluster back trajectories using 2000 parcels ending on (a and b) 15 February 2002 at Reunion, between 9.5 and 10.5 km, and (c and d) 19 February between 8 and 9 km at 1200 UT. Corresponding latitude-longitude positions and their altitude are given by the color scale on the right.

western vicinity of the cyclone (not shown) persists until 19 February (0000 UT), suggesting a PV destruction on 19 February. The signature of ozone intrusions from the stratosphere into the troposphere is still visible on the ozone profile, although the PV filament disappeared 12 hours before. The persistence of a dry air filament on the 19 February Meteosat image (Figure 7d) corroborates this intrusion. Furthermore, stratospheric air observed in the troposphere can retain its original chemical signature for longer than its thermodynamic signature [*Bithell et al.*, 2000].

[49] Vertical PV cross sections have been plotted (Figure 10) to detect the level to which stratospheric PV filaments penetrate: 330 K on 14 February (Figure 10a), 350 K on 17 February (Figures 10b and 10c). On 17 February the convective tower is clearly identified by high values of PV, produced by diabatic heating and frictional forces occurring around the eye of Guillaume (Figure 10c). In Figure 10c, the stratospheric PV filament is visible on the western edge of Guillaume.

[50] Biomass burning is a possible chemical source of ozone precursors in the tropical troposphere [*Randriambelo et al.*, 2000]. The ESA publishes monthly global fire maps on the Web and the February 2002 map is available on http://dup.esrin.esa.int/ionia/wfa/products/0202ESA02.gif. Most of fires during February 2002 occurred north of the equator in Africa, Central America and Asia. Back trajectories calculated in this case study do not indicate their origins. Very few fires occur in the Southern Hemisphere over South Africa [*Randriambelo et al.*, 1998]. This result is in agreement with previous studies of the biomass burning climatological influence, and we can conclude that in this case study, the photochemical origin of ozone played a minor role, in comparison with dynamical mechanisms.

4.2. Irene Event, November 2000

4.2.1. Observations

[51] Figure 11 depicts ozone, temperature and relative humidity profiles obtained by radiosoundings at Irene on

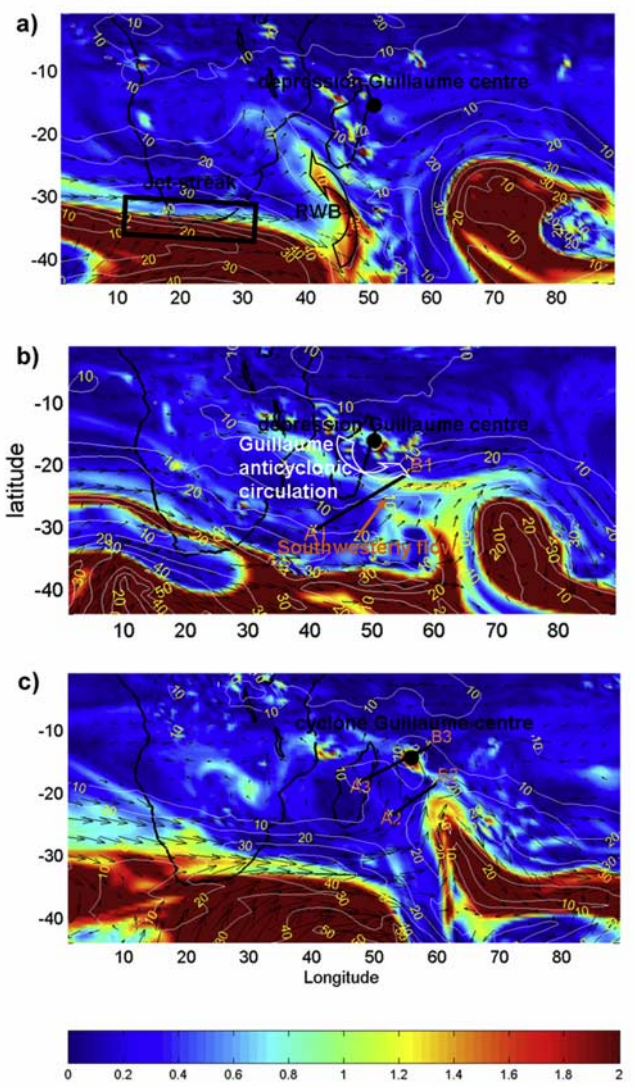

Figure 9. ECMWF potential vorticity (absolute value) on the 340 K isentropic surface on (a) 12 February 2002, (b) 14 February 2002 at 1200 UT, and (c) 17 February 2002 at 0600 UT. Horizontal wind direction and intensity (m s^{-1}) have been superimposed. The lines A and B indicate the limits of the vertical cross sections shown in Figure 10.

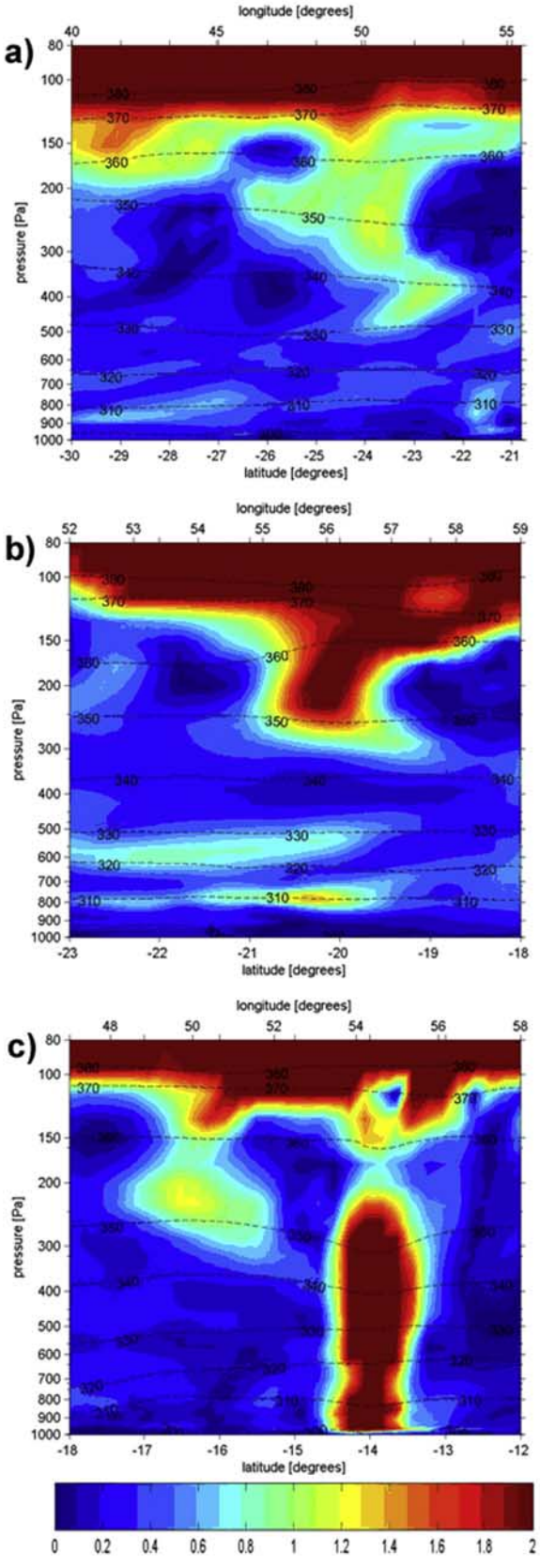

Figure 10. Potential vorticity (absolute value) vertical cross section whose trace is marked on Figure 9. (a) A1B1, (b) A2B2, and (c) A3B3. The potential temperature contours have been superimposed.

11 November 2000. The ozone profile is superimposed on the November climatological profile at Irene.

[52] The ozone profile presents very different characteristics from those obtained for the Guillaume case study. Between the ground and 8 km, ozone values are between 40 and 70 ppbv, within the climatological variability. Between 9 and 14 km (330 K to 370 K), extremely high ozone values (more than 100 ppbv) are observed, with two peaks reaching 170 ppbv. One, located at 10.5 km is a very thin enriched ozone layer and the other is larger, between 12 km and 12.5 km. These values are considerably higher than the climatological mean. The enriched ozone layer is capped by a temperature inversion based at ~13 km (Figure 11b). Another slight variation is visible on the temperature profile near an altitude of 11.5 km. It could be caused by the warming of the atmosphere by ozone. The thermal tropopause is very high (18 km), which is unusual for a site at this latitude (25°S).

[53] The humidity profile is characterized by large values in the lower part of the profile, reaching 90% at 3 km, and above this a layer with 40% relative humidity between 3 and 4 km is observed. The air is dry above 4 km (10–20% RH between 4 and 12 km), exhibiting a rather noisy profile in the free troposphere. A wetter layer (40% between 12 and 14 km) caps the ozone enriched layer observed between 10 and 13 km. Above 15 km, the air is dry again.

4.2.2. Synoptic Situation

[54] As in the Guillaume case study, a convective zone and a jet front system are in the region, but the situation is different (Figure 12). The convective zone is in the Mozambique Channel, and the jet front system is situated to the southwest in the South Atlantic Ocean. The ITCZ is well developed over the central African continent, but far from the measurement point. A large area between 0 and 40°E, and north of 10°S is very cloudy and wet.

[55] On the water vapor Meteosat image (Figure 12b), two dry areas appear: one is close to the upper level front, at 0°E longitude, and 20 to 40°S; the other is larger, near 20°S, 20°E, in the vicinity of the convective area. The second area is larger and drier (darker on the water vapor Meteosat image) than the former area near the front, and also drier than the area near Guillaume, seen in the preceding case study.

4.2.3. Temporal Evolution of the Air Masses

[56] Back trajectories (Figure 13) indicate the short-term origin of the enriched ozone layer: the parcels come from the southwest, and then the west. They have passed through the two dry areas identified on Meteosat images. The long-term origin of the parcels is South America. We note the greater speed of the air parcels, in comparison with the Guillaume case study, due to the influence of the subtropical jet stream.

[57] In the vertical plane, two areas of subsidence are identified, one at −80 hours, which corresponds to the passage of the air parcels over South America (Chili). Many strong vertical perturbations occur in this area, perhaps induced by the mountain chain Cordillere des Andes and by convection. Another area of subsidence is observed between −45 hours and the end point of the trajectories, when the air parcels are between the eastern part of the South Atlantic Ocean and Irene.

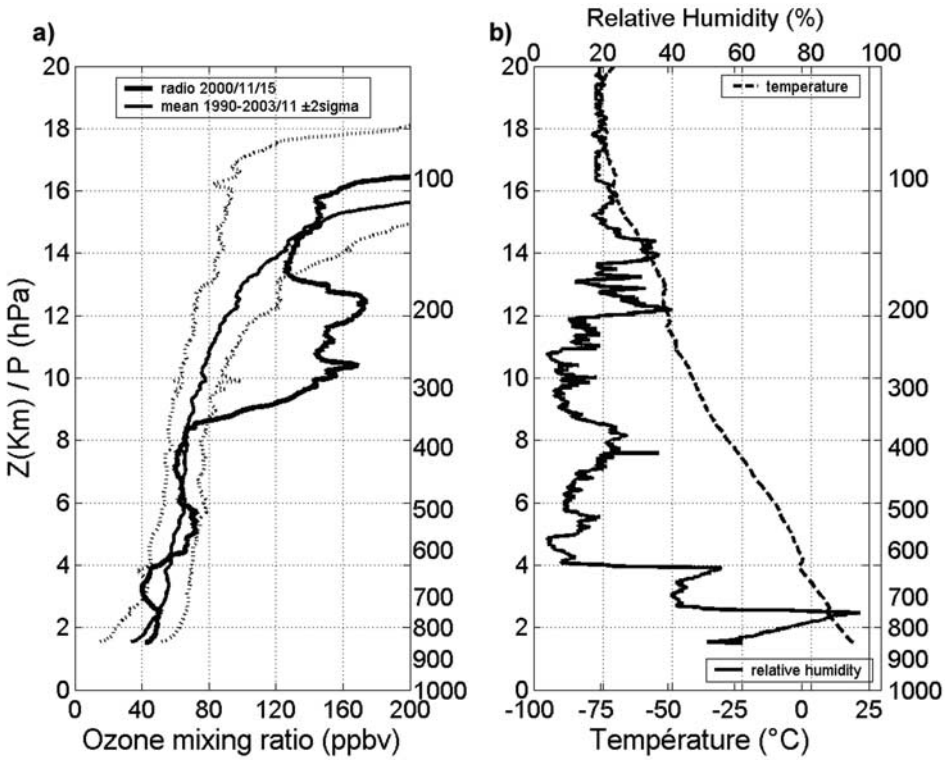

Figure 11. (a) Vertical profiles of ozone mixing ratio obtained by radiosounding over Irene on 15 November 2000 at 0600 UT, superimposed with a climatological profile of ozone for November (24 profiles between 1990 and 2003) and its standard deviation (dashed lines). (b) Vertical profiles of relative humidity and temperature.

[58] PV cross-sectional fields (Figure 14) confirm the stratospheric origin of the dry area near Irene, and the other near the upper level front, visible between 0 and 15°E on 15 November, and which was situated between 25°W and 0° longitude on 13 November (not shown).

[59] If we compare this case study to the preceding one (Guillaume), we find here evidence of important STE signatures (very high ozone and PV values).

[60] In fact, the dry area observed near the convective area is an upper level depression containing stratospheric air, fed by the filament around the convective area in the Mozambique Channel. This case shows some similarities to a previous study of a cutoff low (COL) over South Africa [*Baray et al.*, 2003]. The radiosounding performed on 1 October 1996 in Reunion presents an ozone peak with magnitude and height comparable to the present case study. The main difference between the synoptic situations of the two cases is the role of the convective system (not present in October 1996, present in November 2000) in the stratospheric filamentation and COL formation.

[61] The vertical cross section (Figure 15) shows that the deformation of the PV field reaches the level 330 K. Near

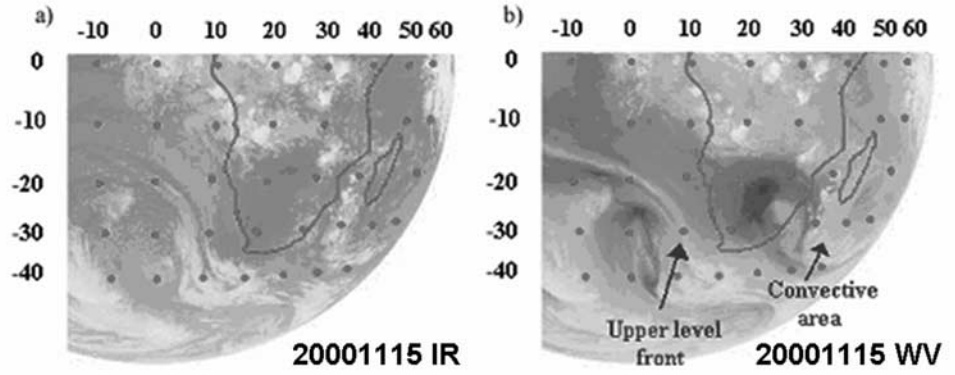

Figure 12. Meteosat-7 image on 15 November 2000 at 0600 UT in the (a) infrared and (b) water vapor channels.

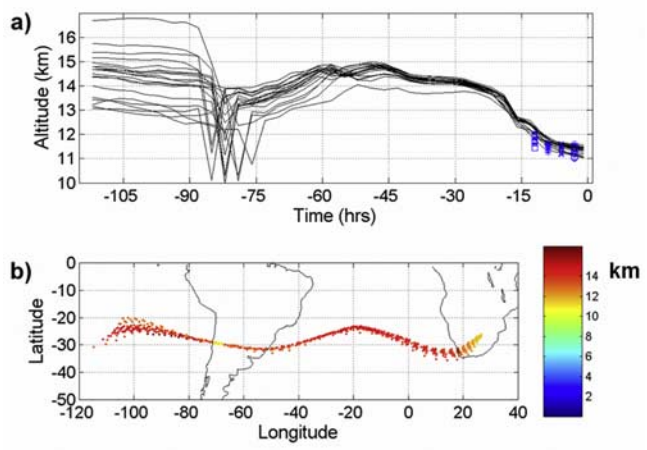

Figure 13. Cluster back trajectories using 2000 parcels ending on 15 November 2000 at 0600 UT over Irene (South Africa) between 11 and 13 km. Corresponding latitude-longitude positions and their altitude are given by the color scale on the right.

the PV anomaly, the isentropic surface 330 K presents important slopes, suggesting frontogenesis mechanisms near the COL. The detachment of the COL in the vertical plan is in progress, but not completed on 15 November 2000.

[62] In November, biomass burning is a possible source for tropospheric ozone in the Southern hemisphere [*Randriambelo et al.*, 1998]. The ESA fire map for November 2000 (available at http://dup.esrin.esa.int/ionia/wfa/products/0011ESA02.gif) shows that few fires occur in South Africa, but some fires occur in South America, where some strong vertical perturbations have been observed on back trajectories. In addition to dynamical sources of ozone (STE), they could contribute to the ozone peak.

[63] In summary, dynamical and chemical mechanisms have both had a role to play in this case study. Moreover, the dynamical mechanism is different to the Guillaume case study. The stratospheric filament which developed around the convective zone in the Mozambican channel fed an upper level depression of stratospheric air in the upper troposphere. The size of this depression and its high concentration of ozone produced a strong ozone peak, amplified by two other sources (fires in South America and an upper level front in the Atlantic Ocean).

5. Conclusion

[64] In this study, in order to improve our understanding of the influence of deep convection and tropical cyclones on the vertical distribution of tropospheric ozone, we have presented a statistical overview and dynamical case studies.

[65] The case studies include three distinct situations (depression Guillaume, cyclone Guillaume, and convection at Irene) of STE occurring in the vicinity of deep tropical convection. In each case, a strong interaction between the dynamics of convection, the jet front system and RWB induces the stratosphere to troposphere exchanges. Stratospheric filaments in the upper troposphere have been detected in ECMWF analyses, and are in good agreement with ozone, humidity and temperature observations. This shows that the STE observed in association with tropical cyclone Marlene was not an isolated event, and that the synoptic context is an important influence on the variability of tropospheric ozone signatures.

[66] In the Guillaume case study, filamentation and subsidence occurred in the two configurations: without an ozone peak but a moderate enhancement of ozone in the major part of the free troposphere on 15 February 2002

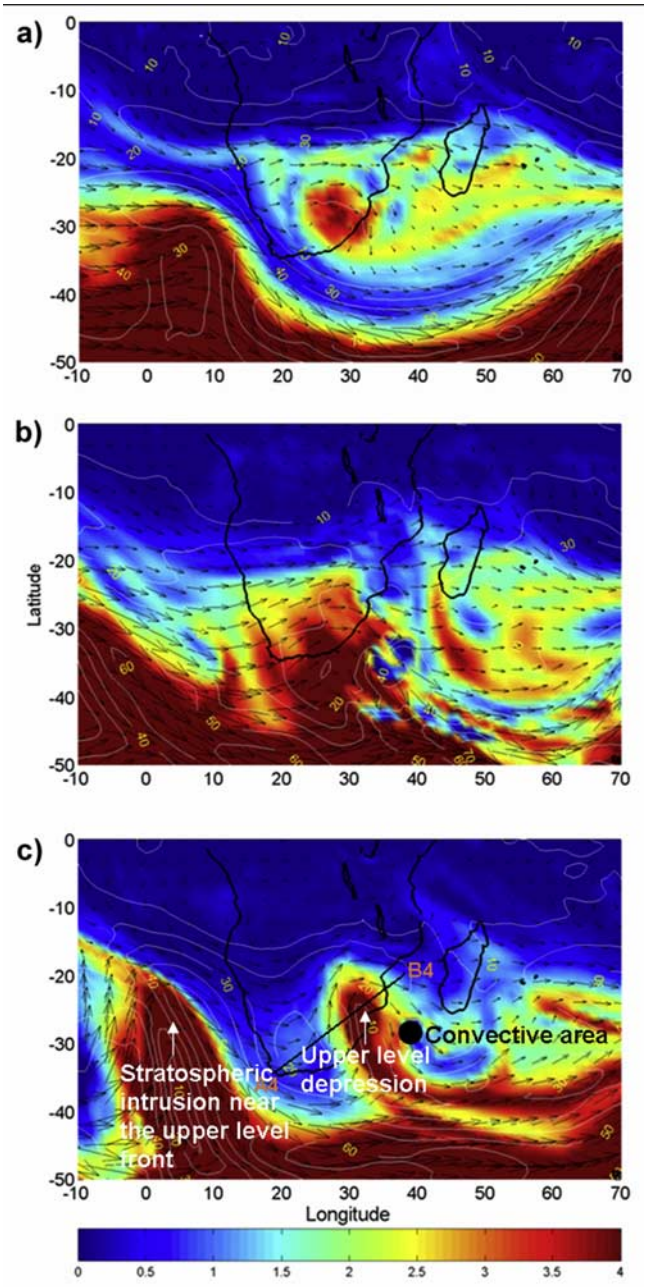

Figure 14. ECMWF potential vorticity (absolute value) on the 350 K isentropic surface on (a) 11 November 2000, (b) 13 November 2000, and (c) 15 November 2000 at 1200 UT. Horizontal wind and geopotential height have been superimposed. A-B indicates the limits of the vertical cross section shown in Figure 15.

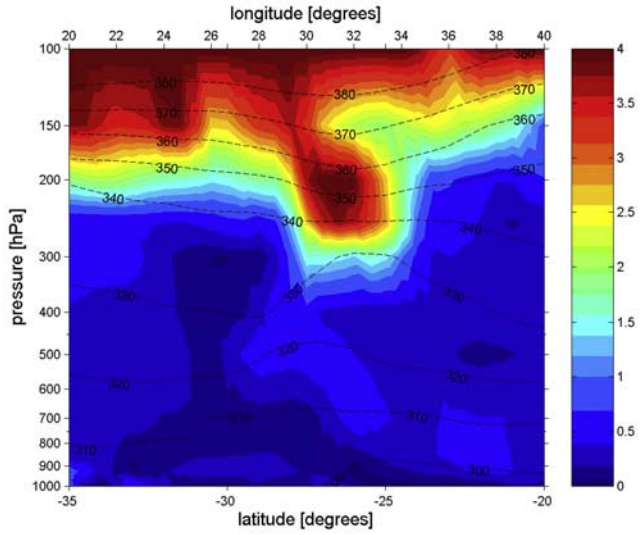

Figure 15. Potential vorticity (absolute) vertical cross section whose trace is marked on Figure 14. The potential temperature (K) contours have been superimposed.

(depression), and with a 100 ppbv ozone peak on 19 February 2002 (cyclone).

[67] In the Irene case study, a large upper level depression coming from the stratosphere, fed by a filament around the divergent zone above the convective area in the Mozambican channel, induced an ozone peak of larger magnitude (170 ppbv) on 15 November 2000. Moreover, secondary ozone sources (a jet front system above the Atlantic and biomass burning in South America) could amplify this ozone enhancement. The radiosounding showed strong ozone enrichment in the upper troposphere, without a signature of pumping from the lower layers, in contrast to the Guillaume case study.

[68] Present observations show that not only cyclones but also cases of deep convection are likely to induce exchanges of air masses between the lower stratosphere and the upper troposphere, especially when deep convection interacts with the subtropical jet stream. Moreover, we have observed that the respective contributions of dynamical components of the interaction at the origin of the ozone intrusion can vary considerably.

[69] The climatological analysis from the Reunion database suggests that the cyclonic mean ozone profile, formed from profiles influenced by cyclones, is characterized by above average ozone values in the mean troposphere. In the upper troposphere the reverse behavior is observed.

[70] This climatological result, with regard to the dynamical elements shown in the case studies, is consistent with the hypothesis put forward at the end of section 3: a dual influence of the convective systems (tropical storms, depressions and cyclones) on the climatology of tropospheric ozone: transfer of ozone from the stratosphere to the midtroposphere and a pumping of ozone-poor air masses from the boundary layer to the upper troposphere.

[71] To further diagnose the fine structure of the upper level interactions associated with convection-induced STE, mesoscale model studies are necessary. Owing to a better resolution, model analyses are actually expected to lead to an improved evaluation of STE induced by deep convection.

[72] **Acknowledgments.** The Laboratoire de Physique de l'Atmosphère is supported by the Centre National de la Recherche Scientifique (CNRS)/Institut National des Sciences de l'Univers (INSU) and the Conseil Régional de La Réunion. Authors are thankful to the ECMWF center for making access to the archived data, to Andreas Stohl for providing the FLEXPART model and Eumetsat for providing the Meteosat data. We thank Françoise Posny and Jean-Marc Metzger for the two balloon launches during the Guillaume event, which were supported by the Programme National de Chimie Atmosphérique (PNCA). We acknowledge Thierry Lin-Chan for his preliminary work on the Irene case study and also Serge Baldy for helpful discussions and suggestions.

References

Baldy, S., G. Ancellet, M. Bessafi, A. Badr, and D. L. S. Luk (1996), Field observation of the vertical distribution of tropospheric ozone at the island of Reunion (southern tropics), *J. Geophys. Res.*, *101*, 23,835–23,849.

Baray, J. L., G. Ancellet, T. Randriambelo, and S. Baldy (1999a), Tropical cyclone Marlene and stratosphere-troposphere exchange, *J. Geophys. Res.*, *104*, 13,953–13,970.

Baray, J. L., J. Leveau, J. Porteneuve, G. Ancellet, P. Keckhut, F. Posny, and S. Baldy (1999b), Description and evaluation of a tropospheric ozone lidar implemented on an existing lidar in the southern subtropics, *Appl. Opt.*, *38*, 3817–6808.

Baray, J. L., T. Randriambelo, S. Baldy, and G. Ancellet (2001), Comment on "Tropospheric O_3 distribution over the Indian Ocean during spring 1995 evaluated with a chemistry-climate model" by A. T. J. de Laat et al., *J. Geophys. Res.*, *106*, 1365–1368.

Baray, J. L., S. Baldy, R. D. Diab, and J. P. Cammas (2003), Dynamical study of a tropical cut-off low over South Africa, and its impact on tropospheric ozone, *Atmos. Environ.*, *37*, 1475–1488.

Barnes, R. A., A. R. Bandy, and A. L. Torres (1985), Electrochemical concentration cell ozonesonde accuracy and precision, *J. Geophys. Res.*, *90*, 7881–7887.

Bethan, S., G. Vaughan, and S. J. Reid (1996), A comparison of ozone and thermal tropopause heights and the impact of tropopause definition on quantifying the ozone content of the troposphere, *Q. J. R. Meteorol. Soc.*, *122*, 928–944.

Bithell, M., G. Vaughan, and L. J. Gray (2000), Persistence of stratospheric ozone layers in the troposphere, *Atmos. Environ.*, *34*, 2563–2570.

Browell, E. V., et al. (1996), Ozone and aerosol distributions and air mass characteristics over the South Atlantic Basin during the burning season, *J. Geophys. Res.*, *101*, 24,043–24,068.

Chatfield, R. B., and P. J. Crutzen (1984), Sulfur dioxide in remote oceanic air: Cloud transport of reactive precursors, *J. Geophys. Res.*, *89*, 7111–7132.

Cooper, O. R., J. L. Moody, D. D. Parrish, M. Trainer, J. S. Holloway, G. Hübler, F. C. Fehsenfeld, and A. Stohl (2002), Trace gas composition of midlatitude cyclones over the western North Atlantic Ocean: A seasonal comparison of O_3 and CO, *J. Geophys. Res.*, *107*(D7), 4057, doi:10.1029/2001JD000902.

Crutzen, P. J., L. E. Heidt, J. P. Krasnec, W. H. Pollock, and W. Seiler (1979), Biomass burning as a source of atmospheric gases CO, H_2, N_2O, NO, CH_3Cl, and COS, *Nature*, *282*, 253–256.

De Laat, A. T. J., M. Zachariasse, G. J. Roelofs, P. van Velthoven, R. R. Dickerson, K. P. Rhoads, S. J. Oltmans, and J. Lelieveld (1999), Tropospheric O_3 distribution over the Indian Ocean during spring 1995 evaluated with a chemistry-climate model, *J. Geophys. Res.*, *104*, 13,881–13,893.

Diab, R. D., et al. (1996), Vertical ozone distribution over southern Africa and adjacent oceans during SAFARI-92, *J. Geophys. Res.*, *101*(D19), 23,823–23,834.

Diab, R. D., A. M. Thompson, K. Mari, L. Ramsay, and G. J. R. Coetzee (2004), Tropospheric ozone climatology over Irene, South Africa, from 1990 to 1994 and 1998 to 2002, *J. Geophys. Res.*, *109*, D20301, doi:10.1029/2004JD004793.

Dickerson, R. R., et al. (1987), Thunderstorms: An important mechanism in the transport of air pollutants, *Science*, *235*, 460–465.

Emanuel, K. A., and M. Zivkovic-Rothman (1999), Development and evaluation of a convection scheme for use in climate models, *J. Atmos. Sci.*, *56*, 1766–1782.

Fishman, J., C. E. Watson, J. C. Larsen, and J. A. Logan (1990), Distribution of tropospheric ozone determined from satellite data, *J. Geophys. Res.*, *95*, 33,599–36,117.

Folkins, I., and C. Appenzeller (1996), Ozone and potential vorticity at the subtropical tropopause break, *J. Geophys. Res.*, *101*, 18,787–18,792.

Fujiwara, M., K. Kita, S. Kawakami, T. Ogawa, N. Komala, S. Saraspriya, and A. Suripto (1999), Tropospheric ozone enhancements during the Indonesian forest fire events in 1994 and in 1997 as revealed by ground-based observations, *Geophys. Res. Lett.*, *26*, 2417–2420.

Gettelman, A., and P. M. De F. Forster (2002), Climatology of the tropical tropopause layer, *J. Meteorol. Soc. Jpn.*, *80*, 911–924.

Gouget, H., J. P. Cammas, A. Marenco, R. Rosset, and I. Jonquières (1996), Ozone peaks associated with a subtropical tropopause fold and with the trade wind inversion: A case study from the airborne campaign TROPOZ II over the Caribbean in winter, *J. Geophys. Res.*, *101*, 25,979–25,993.

Gray, W. M. (1979), Hurricanes: Their formation, structure and likely role in tropical circulation, in *Meteorology Over the Tropical Oceans*, pp. 155–218, R. Meteorol. Soc., Reading, U. K.

Hoskins, B. J. (1991), Towards a PV-θ view of the general circulation, *Tellus*, *43*, 27–35.

Loring, R. O., Jr., H. E. Fuelberg, J. Fishman, M. V. Watson, and E. V. Browell (1996), Influence of a midlatitude cyclone on tropospheric ozone distributions during a period of TRACE A, *J. Geophys. Res.*, *101*, 23,941–23,956.

McBride, J. (1995), Global perspectives on tropical cyclones, *TD 693 TCP 38*, pp. 63–105, World Meteorol. Organ., Geneva, Switzerland.

Mitra, A. P. (1996), Troposphere-stratosphere coupling and exchange at low latitude, *Adv. Space Phys.*, *17*, 1189–1197.

Postel, G. A., and M. H. Hitchman (1999), A climatology of Rossby wave breaking along the subtropical tropopause, *J. Atmos. Sci.*, *56*, 359–373.

Poulida, O., R. R. Dickerson, and A. Heymsfield (1996), Stratosphere-troposphere exchange in a midlatitude mesoscale convective complex: 1. Observations, *J. Geophys. Res.*, *101*, 6823–6836.

Randriambelo, T., S. Baldy, M. Bessafi, M. Petit, and M. Despinoy (1998), An improved detection and characterization of active fires and smoke plumes in south-eastern Africa and Madagascar, *Int. J. Remote Sens.*, *19*(14), 2623–2638.

Randriambelo, T., J. L. Baray, and S. Baldy (2000), Effect of biomass burning, convective venting, and transport on tropospheric ozone over the Indian Ocean: Reunion Island fields observations, *J. Geophys. Res.*, *105*, 11,813–11,832.

Réchou, A., J. L. Baray, S. Baldy, and T. Portafaix (2002), Influence of deep convection on the injection of ozone into the troposphere (stratosphere-troposphere exchange), paper presented at 21st International Laser Radar Conference, Int. Assoc. of Meteorol. and Atmos. Phys., Quebec City, Que., Canada.

Rodgers, E. B., J. Stout, J. Steranka, and S. Chang (1990), Tropical cyclone-upper atmospheric interaction as inferred from satellite total ozone observations, *J. Appl. Meteorol.*, *29*, 934–954.

Scott, R. K., J. P. Cammas, P. Mascart, and C. Stolle (2001), Stratospheric filamentation into the upper tropical troposphere, *J. Geophys. Res.*, *106*, 11,835–11,848.

Stenchikov, G., R. R. Dickerson, K. Pickering, W. Ellis, B. Doddridge, S. Kondragunta, O. Poulida, J. Scala, and W. K. Tao (1996), Stratosphere-troposphere exchange in a midlatitude mesoscale convective complex: 2. Numerical simulations, *J. Geophys. Res.*, *101*, 6837–6851.

Stohl, A., and T. Trickl (1999), A text example of long-range transport: Simultaneous observation of ozone maxima of stratospheric and North American origin in the free troposphere over Europe, *J. Geophys. Res.*, *104*, 30,445–30,462.

Stohl, A., M. Hittenberger, and G. Wotawa (1998), Validation of the Lagrangian particle dispersion model FLEXPART against large scale tracer experiment data, *Atmos. Environ.*, *32*, 4245–4264.

Thompson, A. M., K. E. Pickering, D. P. McNamara, M. R. Schoeberl, R. D. Hudson, J. H. Kim, E. V. Browell, V. W. J. H. Kirchhoff, and D. Nganga (1996), Where did tropospheric ozone over southern Africa and the tropical Atlantic come from in October 1992? Insights from TOMS, GTE/TRACE-A and SAFARI-92, *J. Geophys. Res.*, *101*, 24,251–24,278.

Thompson, A. M., et al. (2003), Southern Hemisphere Additional Ozonesondes (SHADOZ) 1998–2000 tropical ozone climatology: 1. Comparison with Total Ozone Mapping Spectrometer (TOMS) and ground-based measurements, *J. Geophys. Res.*, *108*(D2), 8238, doi:10.1029/2001JD000967.

Wang, C., P. J. Crutzen, and V. Ramanathan (1995), The role of a deep convective storm over the tropical pacific ocean in the redistribution of atmospheric chemical species, *J. Geophys. Res.*, *100*, 11,509–11,516.

G. Ancellet, Service d'Aéronomie, CNRS-UMR 7620, Boite 102, Université Pierre et Marie Curie, 4 Place Jussieu, F-75252 Paris Cedex 05, France.

J. L. Baray, J. Leclair De Bellevue, and A. Réchou, Laboratoire de l'Atmosphère et des Cyclones, CNRS-UMR 8105, Université de La Réunion, 15 Av. René Cassin, BP 7151, F-97715 Saint-Denis Messag Cedex 9, La Réunion, France. (j.ldb@univ-reunion.fr)

R. D. Diab, School of Environmental Sciences, Howard College Campus, University of KwaZulu-Natal, Durban 4041, South Africa.